Delayed Fracture in Fiber Bundles

Author: Antoni Merin Busquets, amerinbu7@alumnes.ub.edu
Facultat de Física, Universitat de Barcelona, Diagonal 645, 08028 Barcelona, Spain.

Advisor: José Manuel Ruiz Franco, jmruizfranco@ub.edu

Abstract: Fracture is usually associated with the application of stresses or strains exceeding a critical rupture threshold, often referred to as the rupture point. However, many materials can fail after a finite stochastic time under a constant subcritical strain, known as delayed fracture. In this work, we study this phenomenon by performing numerical simulations of a one-dimensional fiber bundle model under constant strain, with the aim of developing a model capable of reproducing delayed fracture. We observe that, within a limited strain range, delayed fracture can occur in this type of model if we introduce a continuous damage rule and a local stiffness redistribution.
Keywords: Deformation, elasticity, damage, fracture, simulations.
SDGs: 4: Quality education, 9: Industry, innovation, and infrastructure, 12: Responsible consumption and production, and 13: Climate action.

I. INTRODUCTION

Mechanical failure in solid materials corresponds to a partial or complete degradation of their capacity to support mechanical loads. In the most common case, the failure occurs at the material's fracture threshold. However, some materials can fracture after a finite stochastic time at a constant strain below the threshold value. This phenomenon, known as delayed fracture, occurs without visible macroscopic warning signs and manifests as a catastrophic failure. Therefore, understanding why and how this kind of fracture occurs is crucial in order to avoid the unexpected degradation and failure of critical materials, which can lead to safety risks or reduced material efficiency.

This behavior has been studied experimentally [1, 2] and numerically [1, 3]. It has been found that a pre-fracture deformation zone appears because of a localized damage process and that the exponential growth of this deformation zone culminates in a crack nucleation followed by failure of the system. However, there is still no general framework to understand the microscopic mechanisms that govern delayed fracture and the associated damage process. Therefore, developing a feasible model can be a first step toward a mean-field theory to understand the delayed fracture. For this reason, we study it using a numerical simulation of a one-dimensional fiber bundle model, which corresponds to a finite number of parallel elastic fibers. We note that lattice models [1], spring models [4], as well as most of the other proposed models [5], have more parameters and complex interactions, making it more difficult to characterize the main behavior, while it is well known that fiber bundle models have been successful in studying fractures in solid materials [6] and in developing mean-field theories. Moreover, their low computational cost is noteworthy.

Nevertheless, this model exhibits some limitations due to the difficulty of understanding the direct correlation between a one-dimensional model and the two- and three-dimensional real systems. Moreover, there are very few reported simulations of the delayed fracture phenomenon with fiber bundle models [3], and most of these models have focused on studying the creep rupture under constant stress, the stress-strain curve imposing a deformation rate, or the stress relaxation under constant strain [6, 7].

In this work, we study the main characteristics of the model proposed by S. Zapperi *et al.* [7] with the same parameter values used by J. Sprakel *et al.* [1] adapted directly to a one-dimensional model but redistributing the stiffness at nearest neighbors, thus observing the delayed fracture behavior under some specific conditions.

This work is structured as follows: in Section II we describe the main details of the numerical model, emphasizing how we redistribute the stiffness. In Section III we discuss the main results obtained for a system under constant strain and analyze uniaxial deformations to identify the strain range associated with delayed fracture. Finally, in Section IV, we summarize our findings, and we propose future lines of research to move toward a general framework that explains delayed fracture.

II. MODEL

A. Simulation details

We consider N parallel fibers on a one-dimensional array and suppose all the fibers are always elastic so the force supported by the fiber i at the iteration j follows Hooke's law:

$$f_i^j = \mu_i^j \Delta l_i^j. \tag{1}$$

where μ_i^j denotes the spring constant, and $\Delta l_i = l_i^j - l_0$, with l_i^j the fiber length and l_0 the equilibrium bond length. Every fiber has an associated threshold force $f_{i,thr}$. Therefore, when a fiber has $f_i > f_{i,thr}$, it is prone to weakening, and, specifically, the fiber with the maximum quotient $f_i/f_{i,thr}$ is the only one weakened at that

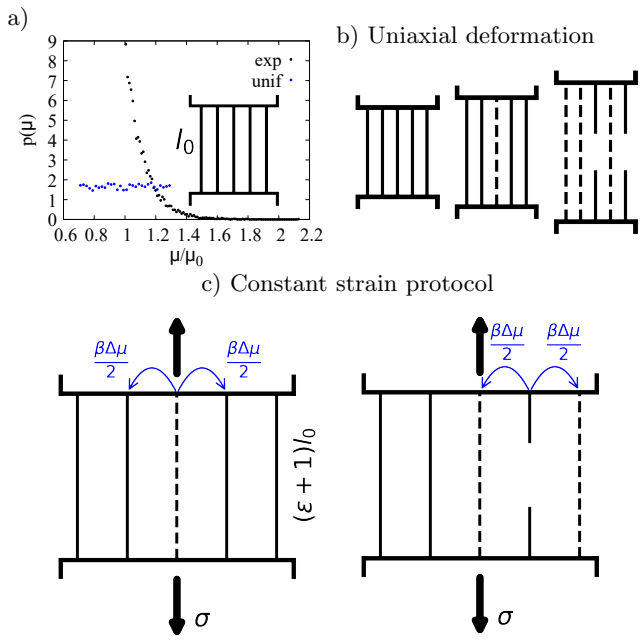

FIG. 1: **(a)** Normalized simulated distribution of the stiffness, for a uniform distribution with $d\mu = 0.3\mu_0$ (blue dots), and for an exponential distribution with $\lambda = 9/\mu_0$ (black dots), generated with $N = 10000$. Inset: Scheme of the fibers in its natural state. **(b)** Scheme of the fibers under increasing uniaxial deformation allowing to stabilize at every step. **(c)** Scheme of the stiffness redistribution after a softening (left) and after a breakage (right) at a constant uniaxial deformation ϵ. Dashed lines indicate that the fiber has undergone some softening.

step (i.e. only one fiber can be softened or broken every step). However, the fiber breaks when it is weakened the n_{soft}-th time, and therefore that fiber no longer supports any force (see Section A of the Supplementary Material for an example illustrating the force behavior of a single fiber). Note that softening and breakage of the fibers are irreversible.

In order to simulate a continuous damage procedure and, therefore, to take into account internal reorganization of the fibers that are suffering, we change its stiffness by applying an α factor when the k-fiber is softened:

$$\mu_k^{j+1} = \alpha\mu_k^j \quad , \quad 0 < \alpha < 1, \tag{2}$$

and also we change the force threshold of that fiber,

$$f_{k,thr}^{j+1} \sim U(\alpha^{d_i} f_{k,thr}^j, f_{thr,0}), \tag{3}$$

with $U(a,b)$ being a uniform distribution (a,b), where $f_{thr,0}$ is the initial threshold, which is equal for all the fibers, and where d_i is the number of times that the i-fiber has been weakened (with the last softening included). Therefore, we are doing the so-called annealed disorder [7], which has been shown to model microscopic rearrangements.

In all the simulations we choose the same parameters as J. Sprakel *et al.* [1]: $f_{thr,0} = 0.35\mu_0 l_0$, $n_{soft} = 20$ and $\alpha = 0.95$, and we use normalized units μ_0 and l_0. However, to create initial inhomogeneities, we generate the initial fibers stiffnesses using a probability density function. Concretely, we explore the uniform distribution $\mu \sim U(\mu_0 - d\mu, \mu_0 + d\mu)$ with different $d\mu$ and the exponential distribution $(\mu - \mu_0) \sim Exp(\lambda)$, see Fig. 1(a). Furthermore, we associate a time to every step of the simulation supposing that between two steps the time increases by a quantity dt distributed exponentially with $dt/t_0 \sim Exp(R_{\text{tot}})$, with R_{tot} denoting the force excess of the system defined as

$$R_{\text{tot}} = \sum_{i\in\phi} \frac{f_i}{f_{i,thr}}, \tag{4}$$

where ϕ is the set of unbroken fibers. Therefore, we are supposing that the softening and breakage events follow a Poisson process over time and, consequently, the time between events follows an exponential distribution. Additionally, we are assuming that the progression of physical time is proportional to the force excess, with a constant proportionality t_0, consistent with the approach described by J. Sprakel *et al.* [1].

Using this model, we have developed two simulations controlling the strain $\epsilon = \Delta l/l_0$: (i) increasing uniaxial strain, as sketched in Fig. 1(b), and (ii) holding the strain constant, as represented in Fig. 1(c). We increase the strain, letting the system stabilize at every small step $d\epsilon$; that is, at every step we let soften or eventually break all the fibers that have to do so. We increase the strain until all the fibers have broken, and at every step we calculate the corresponding stress σ, summing the force over all the fibers:

$$\sigma = \frac{1}{Na_0}\sum_{i=1}^{N} f_i, \tag{5}$$

which also corresponds to the external stress required to maintain the system at strain ϵ, and where $a_0 \sim l_0^2$ is the effective area associated with every single fiber.

To perform the simulation at constant strain, we observe that no fiber breaks if the strain is below the critical strain, and, therefore, we need to introduce some redistributions after every softening or breakage to allow fracture at these strains. We can note that the nearest fibers to the weakened one carry momentarily more load than the rest, trying to stretch out (until the system stabilizes again at a new σ), but, as the strain is fixed, the fiber needs to reorganize internally and therefore increases its effective stiffness. For this reason, we propose a local stiffness redistribution to the nearest unbroken neighbors when the k-fiber weakens:

$$\mu_{\text{sup}}^{j+1} = \mu_{\text{sup}}^j + \beta\frac{\Delta\mu}{2}, \qquad \mu_{\text{inf}}^{j+1} = \mu_{\text{inf}}^j + \beta\frac{\Delta\mu}{2}, \tag{6}$$

where $\Delta\mu = \mu_k^j - \mu_k^{j+1}$ and where sup and inf indicate the nearest unbroken neighbors of the k-fiber, understanding that we are using periodic boundary conditions (the fiber $i = N+1$ is again the first fiber and the fiber with $i = 0$ is the last fiber).

B. Discussion of β-driven stiffness redistribution

The β factor modulates how the stiffness of the nearest neighbors increases and consequently how the stress of the system decreases. We can understand this factor as a way of quantifying how the fibers reorganize internally due to their internal structure, and it therefore acts like the α factor. Both factors can be interpreted in a viscoelastic material as quantities directly related to the stress relaxation time of the entire system.

We see that at every step the stress decreases a quantity:

$$\Delta\sigma = \sigma^{j+1} - \sigma^{j} = \frac{\Delta f_k + \Delta f_{\text{sup}} + \Delta f_{\text{inf}}}{N a_0}. \tag{7}$$

Using Eqs. (2) and (6), we find that if the k-fiber is softened, then:

$$\Delta\sigma = \frac{-(\alpha-1)(\beta-1) f_k^j}{N a_0}, \tag{8}$$

while if the k-fiber is broken:

$$\Delta\sigma = \frac{(\beta-1) f_k^j}{N a_0}. \tag{9}$$

Therefore, we can conclude if *(i)* $\beta > 1$ then the stress grows indefinitely, *(ii)* $\beta = 1$ leads to a constant stress, *(iii)* for $0 < \beta < 1$ the stress decreases, and *(iv)* $\beta = 0$ corresponds to the absence of redistribution, with σ decreasing solely due to the α factor.

III. RESULTS

A. Material response under uniaxial deformations

In a system subjected to uniaxial deformation, as sketched in Fig. 1(b), when all the fibers have the same initial stiffness, i.e. $\mu = \mu_0$, we can analytically derive three distinct strain intervals : *(i)* when $\epsilon \leq f_{thr,0}/(\mu_0 l_0)$ no fiber are weakened, *(ii)* when $\epsilon > f_{thr,0}/(\mu_0 l_0)$ the fibers can be softened and also can break but the probability of breakage is very small until the strain is large enough, and *(iii)* all the fibers are broken when $\epsilon > f_{thr,0}/(\mu_0 l_0 \alpha^{n_{soft}-1}) \approx 0.928$. As a consequence of these strain intervals, we can observe in Fig. 2(a) (black points) the emergence of the following mechanical regimes: *(i)* a linear elastic response of the system, corresponding to the region where no fiber is damaged; *(ii)* a gradual stress decrease as some fibers soften, followed by a more rapid drop in the stress-strain slope once a significant number of fibers begin to break; *(iii)* complete system failure, where the stress drops to zero when the strain becomes sufficiently large. In the following, we denote the yielding point ϵ_y as the strain corresponding to the maximum stress, and ϵ_d as the strain at which at least one fiber can be softened. Therefore, ϵ_d and ϵ_y depend mainly on both the initially maximum and minimum stiffness values of the system and, consequently, on the chosen stiffness distribution. Moreover, we can relate the slope of the initial elastic zone to the Young's modulus, assuming a mean stiffness $\bar{\mu}$:

$$E = \frac{\sigma}{\epsilon} = \frac{\bar{\mu} l_0}{a_0}. \tag{10}$$

This can be deduced directly from Eqs. (1) and (5) and defining $\bar{\mu} = \sum_{i=1}^{N} \mu_i / N$. Therefore, in this case, where all the fibers have the same initial stiffness, $E = \mu_0 l_0 / a_0$.

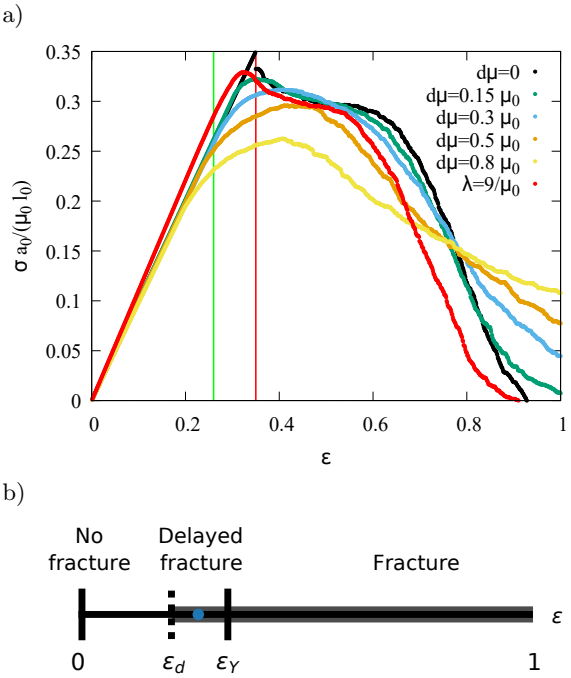

FIG. 2: **(a)** Stress-strain curve for uniform and exponential initial μ distributions. Simulation with $N = 600$ and with steps of increase in the strain, $d\epsilon = 0.001$. The vertical red line marks the $\epsilon_y = 0.35$ value, while the green line marks the $\epsilon = 0.26$ value. **(b)** Diagram with the three main fracture regions observed at constant strain. Scaled according to the result observed with $N = 600$, $\lambda = 9/\mu_0$, and $\beta = 0.95$. The blue point indicates $\epsilon = 0.26$, the value used in Fig. 4.

The three strain intervals also appear if we initialize with a stiffness distribution, but the ϵ values of the regions change because the maximum μ value determines the minimum strain to see some softening or breakage, while the minimum μ value determines the strain for which all the fibers are surely broken. Therefore, we observe the same mechanical regimes, as observed in Fig. 2(a) for the uniform and exponential distributions. However, in these cases, due to system heterogeneity, the stress-strain slope starts to decrease before reaching the maximum stress, and the Young's modulus is, for all the uniform distributions used, $E \approx \mu_0 l_0 / a_0$, while for the exponential distribution $\mathbb{E}[\mu] = \mu_0 + 1/\lambda$, and we used $\lambda = 9/\mu_0$, thus, $E \approx 1.1 \mu_0 l_0 / a_0$. We have used that

$\bar{\mu} \approx \mathbb{E}[\mu]$ when N is large enough. We note that the Young's modulus is greater in the exponential case than in the uniform case, as shown in Fig. 2. In the following, we focus on an exponential stiffness distribution (see Section B of the Supplementary Material for results with a uniform distribution). Unlike the uniform case, the exponential distribution avoids extremely low stiffness values, which would lead to notably flexible fibers, while still allowing for rare, highly stiff fibers.

B. Delayed fracture behavior

Delayed fracture refers to the time-dependent failure of a system held at constant applied subcritical strain, in contrast to conventional fracture, which occurs quasi-instantaneously once the critical strain is exceeded. Within this framework, delayed fracture is characterized by the progressive accumulation of damage over time, eventually leading to macroscopic failure.

Keeping this in mind, if we apply the constant strain protocol sketched at Fig. 1(c), we would observe the delayed fracture only if the applied constant strain is large enough to initially have at least one fiber that can be softened ($\epsilon > \epsilon_d$) and small enough not to exceed the yielding point ($\epsilon < \epsilon_y$), as sketched in Fig. 2b. However, since the process is stochastic, being within this region is not a sufficient condition to observe delayed fracture. This leads to situations in which system failure is not observed, as shown in Fig. 3(d), where we report the fraction of identical independent simulations in which at least one fiber breaks, Φ.

We first explore the scenario in which redistribution is not applied, corresponding to $\beta = 0$. We find that it is not possible to observe delayed fracture behavior for any ϵ or system size. This is because, even if the simulation is initialized with some fibers having a large μ, it ends once all these fibers break or when $f_i < f_{i,thr}$ for all fibers. Therefore, since there is no redistribution, if the initial average fiber force is below the force threshold, only some punctual fibers may break without spreading out the fracture. Moreover, we find that in this case $\epsilon_d = \epsilon_m$, and therefore delayed fracture cannot occur, in agreement with the above arguments. For this reason, in the following we analyze the delayed fracture behavior for $\beta = 0.95$, even though different β values are also expected to produce fracture at constant subcritical strains (see Section C of the Supplementary Material for results with different β values).

When $\epsilon \geq \epsilon_y$, we see the initial fracture of the system after a very small time under the constant strain and we can consider that the system collapses instantaneously, as seen in Fig. 3(a). However, for subcritical strain, the fracture occurs after a finite time. In this case, we can distinguish four main stages characteristic of delayed fracture and relate them to the evolution of the force excess, as shown in Fig. 4 (b) and (c): (I) the stiffest fibers begin to undergo softening, creating localized regions where the damage starts to concentrate; in these regions the fibers have large d_i, implying low force thresholds. Meanwhile, since only softening processes occur, the total excess force tends to decrease similarly to the total stress (see Eq. (8)). Suddenly one of these regions begins to dominate, becoming the most strongly softened. (II) Eventually, one of the fibers in this most damaged region breaks, increasing a lot the stiffness of the nearest fibers and, consequently, the force they support. As a result, these fibers become the most susceptible to breaking. (III) The crack starts to grow around the first broken fiber in both directions, and R_{tot} increases because, even though the system stress decreases (see Eq. (9)), the local force supported by the fibers around the crack is significantly greater than that supported by the other fibers. Taking into account that $dt/t_0 \sim Exp(R_{\text{tot}})$, we note that the time accelerates as the crack advances and, therefore, the speed of crack propagation increases. (IV) Finally, the crack growth rate starts to stabilize because the number of fibers decreases and the stress decay starts to take over again, leading to a more constant force excess, which ultimately goes to zero once all the fibers are broken. Moreover, through Fig. 4 we can understand visually these four stages, seeing how initially some fibers are randomly weakened and a more damaged region starts to appear (I), until a fiber of this more damaged region breaks (II), thereby triggering an avalanche around this fiber (III), and finally propagating through the entire system (IV). These four stages are also observed by the lattice model of J. Sprakel *et al.* [1].

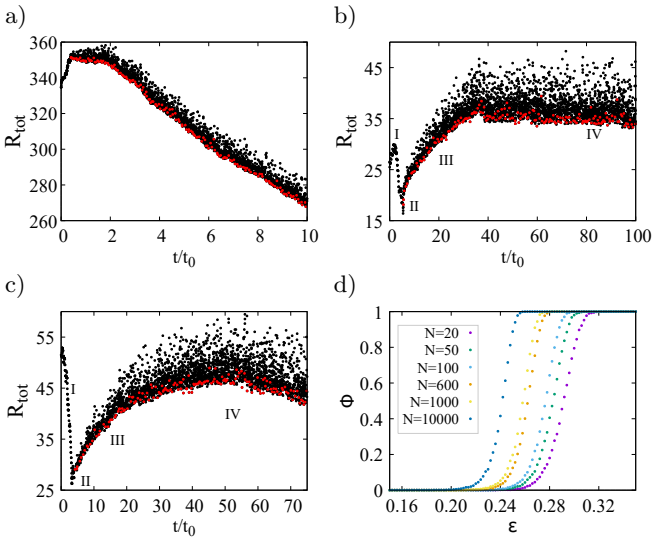

FIG. 3: Evolution of the force excess for constant strains **(a)** $\epsilon_y = 0.326$, **(b)** $\epsilon = 0.260$, and **(c)** $\epsilon = 0.274$. Results with $N = 600$, $\lambda = 9/\mu_0$, and $\beta = 0.95$. The red points highlight when a break occurs. The four main regions are indicated in the figures **(b)** and **(c)**, corresponding to the damage region I, the first break II, the first expansion of the crack III, and the stabilization of the crack expansion IV. **(d)** Fraction of simulations in which at least one fiber breaks at different constant strains. Calculated from 5000 independent simulations with $\beta = 0.95$. Different sizes are represented.

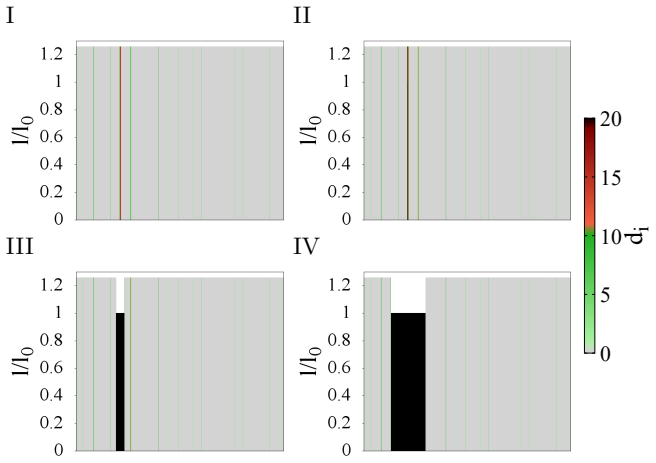

FIG. 4: Delayed fracture simulation time sequence. The four main stages are represented, corresponding to the damage region, $t = 4.5t_0$ (I), the first break, $t = 5.6t_0$ (II), the first expansion of the crack, $t = 20t_0$ (III) and the stabilization of the crack expansion, $t = 60t_0$ (IV). Simulated with $\epsilon = 0.26$, $\beta = 0.95$, $\lambda = 9/\mu_0$, and $N = 600$. All the fibers are represented with the corresponding color according to the number of softening events d_i they have undergone and with their corresponding length. The broken fibers are indicated with length $l = l_0$ and black color.

We also observe these four main stages when delayed fracture occurs on both large and small systems. However, we find that, under the exponential distribution, larger systems experience delayed fracture at smaller strains due to the increased probability of fibers with high initial stiffness as N increases. This is clearly observed by examining Φ, as shown in Fig. 3(d). However, with the uniform distribution, as the maximum stiffness is bounded, for sufficiently large N, the maximum stiffness permitted determines the minimum strain for which we can observe at least one break, as discussed in section III A and with more details in section B of the Supplementary material. Note that, because with $\beta = 0.95$ a fiber breaking usually leads to the failure of the entire system, Φ is similar to the fraction of simulations in which the whole system fails.

IV. CONCLUSIONS

In this work, after examining the fracture with a continuous damage fiber bundle model and observing that delayed fracture does not occur, we propose and analyze a fiber bundle model that reproduces delayed fracture under constant subcritical strain by introducing a stiffness redistribution mechanism to first neighbors. We find that by using this model, the system fails instantaneously if the applied strain is sufficiently large, is unlikely to fracture under low strains, and for intermediate strains, the system may either fail instantaneously, remain intact, or initiate fracture after a finite stochastic time, manifesting the expected delayed fracture behavior in this latter case.

It is worth noting that this model can reproduce the four stages of delayed fracture reported in the lattice model of J. Sprakel *et al.* [1]. These stages are: (I) the formation of a spatial region where damage accumulates, (II) the onset of fracture, (III) the initially accelerated propagation of the crack, and (IV) the stabilization of crack growth.

From the experimental point of view, previous studies have found that the law governing the spatial distribution of damage is a determining factor in delayed fracture behavior, particularly in the time to fracture [2]. Therefore, in future work, it would be interesting to explore alternative stiffness redistribution mechanisms, such as redistribution to second or higher-order neighbors or distance-dependent laws leading to less spatially localized damage. In addition, studying the fiber bundle model with stiffness distributions based on experimental data could be of practical relevance for material design. Finally, an analytical solution is expected for some specific stiffness redistribution mechanisms and remains to be explored.

Acknowledgments

I would like to thank Professor José Manuel Ruiz Franco for his constant dedication and all his advice, as well as thank my family for their encouragement through this project.

[1] H. M. van der Kooij, S. Dussi, G. T. van de Kerkhof, R. A. M. Frijns, J. van der Gucht & J. Sprakel, *Laser Speckle Strain Imaging reveals the origin of delayed fracture in a soft solid.* **4**, eaar1926 (Science Advances, 2018).

[2] J. Ju , G. E. Sanoja, L. Cipelletti, M. Ciccotti, B. Zhu, T. Narita, C. Y. Hui & C. Creton, *Role of molecular damage in crack initiation mechanisms of tough elastomers.* **121**, e2410515121 (Proceedings of the National Academy of Sciences, 2024).

[3] S. Hao, B. Zhang & J. Tian, *Relaxation creep rupture of heterogeneous material under constant strain.* **85**, 012501 (Physical Review E, 2012).

[4] P. K. V. V. Nukala, S. Zapperi & S. Šimunović, *Statistical properties of fracture in a random spring model.* **71**, 066106 (Physical Review E, 2005).

[5] J. Tauber, J. van der Gucht & S. Dussi, *Stretchy and disordered: Toward understanding fracture in soft network materials via mesoscopic computer simulations.* **156**, 160901 (The Journal of Chemical Physics, 2022).

[6] B. K. Chakrabarti, A. Hansen & S. Pradhan, *Failure Processes in Elastic Fiber Bundles.* 3rd. ed. (Review of Modern Physics, 2009).

[7] F. Kun, S. Zapperi & H. J. Herrmann, *Damage in fiber bundle models.* 2nd. ed. **17**, 269-279 (The European Physical Journal B, 2000).

Fractura retardada en feixos de fibres

Author: Antoni Merin Busquets, amerinbu7@alumnes.ub.edu
Facultat de Física, Universitat de Barcelona, Diagonal 645, 08028 Barcelona, Spain.

Advisor: José Manuel Ruiz Franco, jmruizfranco@ub.edu

Resum: La fractura s'associa a l'aplicació de tensions o deformacions per sobre d'un llindar de ruptura crític, sovint anomenat punt de ruptura. Tanmateix, molts materials poden patir el conegut com a fractura retardada, és a dir, es poden trencar després d'un temps finit estocàstic sota una deformació per sota de la crítica. En aquest treball estudiarem aquest fenomen amb la finalitat de desenvolupar un model que reprodueixi la fractura retardada a partir de simulacions numèriques d'un feix de fibres unidimensional sotmès a deformació constant. Observem que, dins d'un rang limitat de deformació, la fractura retardada pot aparèixer en aquest tipus de models si s'hi introdueix una regla de dany continu i una redistribució local de la rigidesa de les fibres.
Paraules clau: Deformació, elasticitat, dany, fractura, simulacions.
ODSs: Aquest TFG està relacionat amb els Objectius de Desenvolupament Sostenible (SDGs)

Objectius de Desenvolupament Sostenible (ODSs o SDGs)

1. Fi de la es desigualtats		10. Reducció de les desigualtats	
2. Fam zero		11. Ciutats i comunitats sostenibles	
3. Salut i benestar		12. Consum i producció responsables	X
4. Educació de qualitat	X	13. Acció climàtica	X
5. Igualtat de gènere		14. Vida submarina	
6. Aigua neta i sanejament		15. Vida terrestre	
7. Energia neta i sostenible		16. Pau, justícia i institucions sòlides	
8. Treball digne i creixement econòmic		17. Aliança pels objectius	
9. Indústria, innovació, infraestructures	X		

Aquest TFG és part d'un grau universitari de Física motiu pel qual es relaciona amb l'ODS 4, i en particular amb les fites 4.3 i 4.4. El contingut del treball també el podem relacionar amb l'ODS 9, concretament les fites 9.1 i 9.5 i amb l'ODS 12, fites 12.2 i 12.5, ja que l'estudi de la fractura retardada intenta contribuir en la fabricació de materials més duraders i segurs. Finalment, de forma indirecta, aquest treball es pot relacionar amb l'ODS 13, específicament la fita 13.1, en la mesura que una millor comprensió dels processos de fractura pot contribuir a millorar la capacitat d'adaptació d'infraestructures a situacions adverses.

GRAPHICAL ABSTRACT

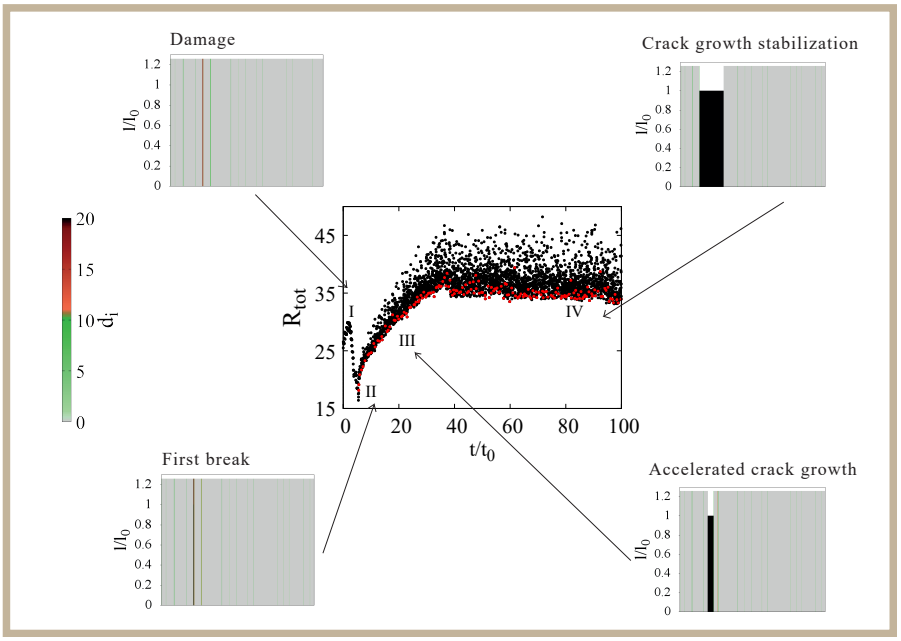

Appendix A: Softening process illustrated

The damage protocol described by Eqs. (2) and (3) can be clearly understood by observing the evolution of the force on a single fiber as the strain is increased in small steps, and by comparing it with the corresponding force threshold at each step. This is illustrated in Fig. 5, where we can see the force drops abruptly when the threshold is reached and then increases again until the new threshold is reached.

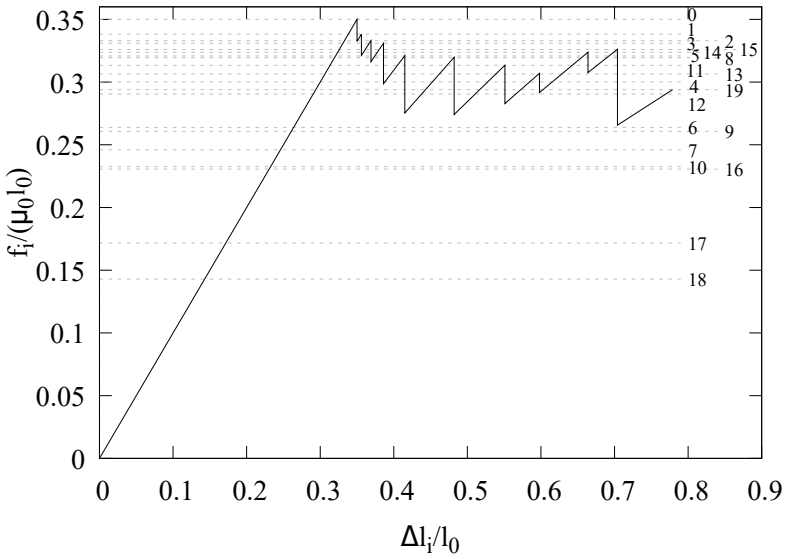

FIG. 5: Force as a function of fiber elongation until the fiber breaks, illustrating the softening process of a randomly chosen fiber in a system of $N = 600$ fibers. Simulation with steps of increase in the strain $d\epsilon = 0.001$. The dashed horizontal lines indicate the evolution of the force thresholds, with the number at the end of each line showing the corresponding d_i for each threshold.

Appendix B: Delayed fracture behavior with uniform stiffness distribution

With a uniform distribution, we can also observe the delayed fracture behavior. However, if $d\mu$ is small, then $\epsilon_d \lesssim \epsilon_Y$, as shown in Fig. 2(a), and thus the range of strains over which we can see delayed fracture is very limited. In Fig. 6(a-c), we can show, through the evolution of the force excess, how delayed fracture emerges at different subcritical strains.

We examine the fraction of simulations in which at least one fiber breaks, Φ, when the simulations are repeated under identical conditions, as shown in Fig. 6(d). Since the maximum stiffness is bounded, fracture cannot occur when $\epsilon < f_{thr,0}/(max(\mu)l_0)$ for any system size. This explains why, for large systems, fracture never occurs below this value and practically always occurs above it.

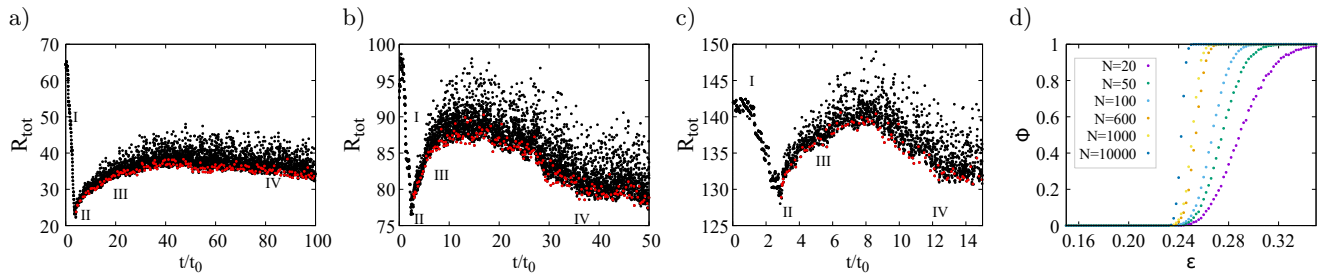

FIG. 6: Initial time evolution of the force excess for constant strains **(a)** $\epsilon = 0.252$, **(b)** $\epsilon = 0.260$, and **(c)** $\epsilon = 0.274$. Results correspond for a system with $N = 600$, $\beta = 0.95$, and uniform distribution with $d\mu = 0.5\mu_0$. The red points highlight when a break occurs. The four main regions are indicated, corresponding to the damage region I, the first break II, the first expansion of the crack III, and the stabilization of the crack expansion IV. **(d)** Fraction of simulations in which at least one fiber breaks at different constant strains. Calculated from 5000 independent simulations, $d\mu = 0.5\mu_0$, and with $\beta = 0.95$. Different sizes are represented.

Appendix C: Delayed fracture behavior for different β values

Performing simulations with different redistribution values shows that delayed fracture occurs for both greater and lower β values. However, it is worth noting that, for lower β values, fracture below ϵ_y is expected only if the stiffness distribution creates inhomogeneities with fibers of sufficiently high stiffness.

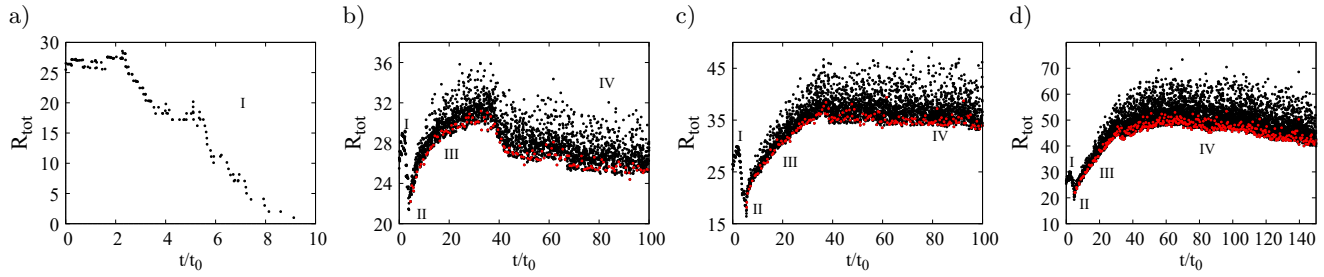

FIG. 7: Initial time evolution of the force excess for different β values **(a)** $\beta = 0.8$, **(b)** $\beta = 0.90$, **(c)** $\beta = 0.95$, and **(d)** $\beta = 0.97$. Results correspond for a system with $N = 600$, constant strain $\epsilon = 0.26$, and exponential stiffness distribution with $\lambda = 9/\mu_0$. The red points highlight when a break occurs. The four main regions are indicated, corresponding to the damage region I, the first break II, the first expansion of the crack III, and the stabilization of the crack expansion IV.

Appendix D: Change of variables method for sampling probability densities

If X is a random variable that follows a uniform distribution $U(0,1)$, and we want a random variable Y defined on the support (a,b) that follows the probability density function $g(y)$, then it satisfies:

$$G(y) - x = 0, \tag{D1}$$

where $G(y) = \int_a^y g(y')dy'$ denotes the cumulative distribution function. Therefore, by solving Eq.(D1), we can find a direct relation between x (a sample of X) and y (a sample of Y), which may be analytical or not.

Some specific cases are:

I) If Y follows a uniform U(a,b) then:

$$y = (a-b)x + b, \tag{D2}$$

II) If Y follows an exponential distribution with parameter γ, then $Y \in [0, \text{inf})$ and:

$$y = -\frac{1}{\gamma} log(x). \tag{D3}$$

In this work, all uniform and exponential random variables were generated using this method and the FORTRAN pseudo-random number generator called *RAND()* to generate random variables following a uniform distribution $U(0,1)$.